Rock and Soil Mechanics 2025 46(8): 2573–2585
https: //doi.org/10.26599/RSM.2024.94300581
ISSN 1000–7598
journal homepage: rocksoilmech.whrsm.ac.cn

Horizontal bearing performance of large-diameter prestressed reinforced concrete pipe pile group

XIE Hong-li, ZHOU-Zhi-jun, REN Yu-bo, TIAN Ye-qing, FAN Jing-can
(School of Highway College, Chang'an University, Shaanxi, Xi'an 710061)

Abstract: This paper presents the findings on the horizontal bearing performance of prestressed reinforced concrete (PRC) pipe pile group. Using field horizontal static load tests, we conducted an analysis and comparison of the horizontal bearing capacity among single piles, single pile caps, and double pile caps, while also investigating the influence of pile caps on the horizontal bearing capacity of the pipe piles. We used the ABAQUS software to compare and analyze the effects of pile group with different pile cap thicknesses, numbers of piles, and pile spacings. The findings show that the horizontal critical load of a double pile cap is twice that of a single pile cap, while the horizontal ultimate load of a double pile cap is 3.095 times that of a single pile cap. An increase in cap thickness increases the bending moment at the pile top. Conversely, there is a slight decrease in the horizontal bearing capacity of the pile group. As the number of piles increases, the mutual influence between adjacent piles decreases, leading to an enhancement in the overall bearing capacity of the pile group. The horizontal bearing capacity of pile groups augments with greater pile spacing. The findings provide a theoretical foundation and serve as a reference for the application of PRC pipe piles in highway bridge engineering.
Keywords: prestressed reinforced concrete (PRC) pipe piles; horizontal static load test; horizontal bearing capacity; pile cap; pile group effect; ABAQUS

1 Introduction

Pile foundations, known for their high bearing capacity and wide applicability, are widely utilized in civil engineering, with a utilization rate exceeding 90%[1-2]. Prestressed reinforced concrete pipe piles (PRC pipe piles) have seen rapid development domestically and internationally, thanks to their high single-pile bearing capacity, short construction period, high automation, good quality, quick forming and curing, and cost-effectiveness[3-4]. They have been extensively utilized in supporting deep foundation pits[5-7] and become a vital pile foundation type in geotechnical engineering, especially in foundation engineering [8-12]. In traditional pile foundation designs, only the vertical load-bearing capabilities are taken into account. Conversely, in new types of structures like long-span and underwater bridges, pile foundations frequently need to accommodate significant horizontal forces, including wind and seismic loads[13]. Thus, the performance of pile foundations under horizontal loads has become a pivotal aspect of structural design[14-15].

Research into the stress-strain mechanisms and deformation behaviors of pile foundations under horizontal loads has consistently been a challenging and popular topic in academic research [16-19]. In prior research, the calculation of the horizontal load capacity of pile groups is merely a basic summation of the horizontal load capacity of individual piles, neglecting the interactions among pile groups[20-21], the lateral resistance provided by large-scale pile caps, and the enhancement of pile group horizontal load capacity, thereby underestimating their ability to withstand horizontal loads and leading to inefficiencies[22-23]. Currently, the principal methods utilized to investigate the horizontal bearing characteristics of pile groups include the pile group efficiency approach, the elastic theory method, the foundation reaction technique, the *p*-*y* (pile side soil resistance - horizontal displacement of pile body) curve method, numerical simulations, and static load tests[24-27]. Numerous engineering practices have demonstrated that horizontal static load tests are the most reliable method for studying the horizontal bearing characteristics of piles[28-29]. In studies examining the horizontal bearing capacity of piles, the significance of pile caps is frequently neglected. Both traditional theoretical analysis methods and field static load testing approaches exhibit numerous shortcomings[30]. Ding and Wang[31] demonstrated that traditional theoretical analysis methods struggled to account for the contribution of the cap to the horizontal bearing capacity of a single pile, leading to substantial errors in the analysis results. Field static load testing demands considerable time and funding, and there is limited existing data on joint testing of pile caps and piles. It is recommended to conduct research and analysis using finite element analysis[32]. Bai[33] analyzed the impact of the size and burial depth of the pile cap on the horizontal bearing capacity of piles using ABAQUS. However, additional analysis and

Received: 24 November 2024 Accept: 18 April 2025
This work was supported by the Shaanxi Provincial Transportation Technology Project (23-72K).
First author: XIE Hong-li, female, born in 1999, PhD candidate, mainly engaged in research on geotechnical engineering. E-mail: 1415405794@qq.com
Corresponding author: ZHOU Zhi-jun, male, born in 1975, PhD, Professor, research interests: geotechnical engineering, bridge engineering.
E-mail: zhouzhijun@chd.edu.cn

engineering verification are required to investigate the effect of pile caps on the horizontal bearing capacity of single piles under various soil conditions.

In the past, numerical analyses, and theoretical research had been conducted on the horizontal bearing capacity of PHC (prestressed high-strength concrete) pipe piles[34-35]. However, relatively little research has been conducted on the horizontal bearing capacity and group effect of PRC pipe piles. Additionally, there is limited research on how pile caps affect the horizontal bearing capacity of pipe piles[36-40]. The pile cap effect in PRC pile foundations is influenced by various factors. Consequently, the quantitative analysis of the pile cap effect in pile group performance is insufficient. Currently, the majority of research on pile cap effects in pile groups concentrates on individual pile behavior or simplified pile group layouts. Neglecting the synergistic interaction between pile caps and adjacent piles in heterogeneous soil conditions[41-44]. Therefore, studying the effect of grouped piles under horizontal loads on PRC pipe piles and the influence of pile caps on the horizontal bearing capacity of pile foundations has become an urgent issue that needs to be addressed in the engineering field. This paper combines field experiments and numerical simulations to investigate the horizontal ultimate bearing capacity and turning moment variations of both single and grouped piles of large-diameter PRC pipe piles, aiming to address the deficiency in research on the horizontal bearing characteristics of such piles.

This paper is based on the field test conducted on Huangxing Village Bridge, located on the Fuzhou-Meizhou Expressway in Zhouzhi County, Xi'an City. By conducting horizontal static load tests, we compared and analyzed the horizontal load-displacement curves of single piles and single pile caps, those of single pile caps and double pile caps, as well as the displacement time logarithmic curve. The objective was to determine the influence of the cap on the horizontal bearing capacity of pipe piles. We used finite element software to analyze the pile group effect of PRC pipe pile foundations considering different cap thicknesses, numbers of piles, and pile spacings. We compared the standard recommendation method with the finite element calculation method for the comprehensive coefficient of group pile effect, thereby providing a theoretical basis for the application design and construction process of PRC pipe piles in bridge engineering.

2 On site testing

2.1 Project overview

The test site is situated at Huangxing Village Bridge on the Fuzhou-Meizhou Expressway in Zhouzhi County, Xi'an City, neighboring County Road X312. The test construction platform is configured in a rectangular shape, measuring 30 m×30 m. In the experiment, seven piles are constructed using C80 concrete, each having an outer diameter of 0.8 m and an inner diameter of 0.54 m. The total lengths of test piles S1-S4 are 40 m, whereas those of S5-S7 are 33 m. Single pile horizontal static load tests are conducted on test piles S1-S5. To assess the influence of pile caps on the horizontal bearing performance of both single and double piles, a horizontal static load test with a single pile cap is conducted on test pile S5. Similarly, a test with a double pile cap is conducted on test piles S6 and S7. The experiment employs a high cap foundation, where the bottom of the cap is level with the ground. The dimensions of the single pile cap are 1.8 m×1.8 m×1.8 m, whereas those of the double pile cap are 1.8 m×4.6 m×1.8 m, featuring a pile spacing of 2.8 m. The paper primarily focuses on test piles S2, S3, and S5-S7, with the pile layout illustrated in Fig. 1.

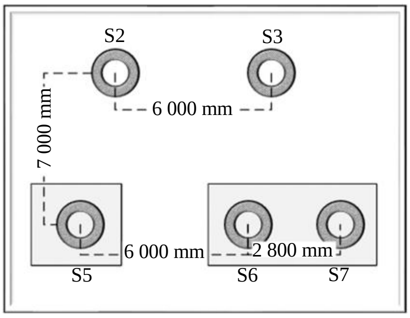

Fig. 1 Pile position layout

Based on field drilling sampling and indoor geotechnical tests, the geological structure and soil layer details of the pipe pile test area are presented in Table 1. The soil layer in the experimental area primarily consists of silty clay having low natural moisture content. In the experimental area, at a depth of 32.4-33.9 m, there exists a round gravel layer, which offers good drainage and enhances the seismic and liquefaction resistance of the pile foundation. PRC pipe piles demonstrate good adaptability in soft soil areas, possessing better bending and shear resistance when compared to cast-in-situ piles of the same cross-section. They meet the unique demands of pile foundations in such areas. In sandy areas, PRC pipe piles exhibit high bearing capacity and deformation resistance. Additionally, PRC pipe piles offer robust support in gravel layers with complex geological conditions. Their construction process is relatively simple, thereby minimizing the impact of construction on the surrounding environment. In summary, PRC pipe piles demonstrate excellent adaptability and significant advantages under various geological conditions. However, in practical applications, emphasis should be placed on construction standards, geological exploration, monitoring, and testing to guarantee construction quality and engineering safety.

Table 1 Physical parameters of on site soil layers

Soil layer	h /m	ρ /(kg · m^{-3})	$E_{s\,(1\text{-}2)}$ /MPa	c /kPa	φ / (°)	q_{ik} /kPa	f_{a0} /kPa
Silty clay	5.0	1 506	7.26	15.624	26.96	50	140
Silty clay	11.0	2 089	4.14	18.538	27.30	55	180
Silty clay	16.4	1 871	10.96	21.217	26.99	50	140
Round gravel	1.5	2 651	35.18	—	39.56	110	380
Silty clay	11.1	1 833	17.59	25.742	30.73	50	140

Note: h = depth; ρ =density; $E_{s\,(1\text{-}2)}$ = compression modulus; c = cohesion; φ = internal friction angle; q_{ik} = standard value of lateral friction resistance; f_{a0} = characteristic value of foundation bearing capacity.

2.2 Experimental plan

A horizontal static load test is conducted on PRC pipe piles using a QF200-20 hydraulic jack (with a measuring range of 200 kN to 2 000 kN) to apply horizontal force to single piles, single pile caps, and double pile caps. To ensure the horizontal load applied by the jacks aligns with the pile body's axis, a spherical hinge is installed at the interface between the jacks and the piles (as shown in Fig. 2). The experiment employs a slow loading method for automatic loading, with a maximum load capacity of 600 kN for single piles and single pile caps. The initial load is 120 kN, with subsequent levels loaded with 60 kN each. For the double pile cap, the maximum load capacity is 1 900 kN, with an initial stage load of 200 kN and incremental loads of 100 kN.

(a) Lifting jack

(b) Single pile cap

(c) Double pile cap

Fig. 2 Horizontal static load test

As per the current national standard, *Technical code for building pile foundations* [45], the equation for calculating the characteristic value of the horizontal bearing capacity of pipe piles is as follows:

$$R_{ha} = 0.75\frac{\alpha^3 EI}{v_x}x_{0a} \tag{1}$$

Where R_{ha} is the characteristic value of the horizontal bearing capacity of a single pile; α is the horizontal deformation coefficient of the pile; EI is the bending stiffness of the pile body; x_{0a} is the allowable horizontal displacement at the top of the pile; v_x is the horizontal displacement coefficient of the pile top.

$$R_h = \eta_h R_{ha} \tag{2}$$

Where R_h is the characteristic value of the horizontal bearing capacity of the pile group; η_h is the comprehensive coefficient of pile group effect.

Based on Eqs. (1) and (2), when the pile top experiences a horizontal displacement of 10 mm, the characteristic horizontal bearing capacity of a single pile is 160.38 kN, while for a group of piles, it is 372.43 kN. The maximum loading capacity for this experiment is calculated at 3-4 times the allowable bearing capacity.

3 Analysis of horizontal static load test

3.1 Horizontal bearing capacity of a single pile

3.1.1 Load bearing performance analysis

The horizontal critical load of a pile is the horizontal load at which the concrete in the tensile zone cracks and ceases to function effectively under gradually increasing horizontal thrust. The horizontal ultimate load is the maximum load a pile can withstand when subjected to horizontal forces. As per the current national standard, *Technical specification for piles testing of highway engineering*[46] the horizontal critical load can be determined based on the horizontal load value of the previous level before the inflection point on the $H_0 - Y_0$ (horizontal load- displacement) curve, and the horizontal load value corresponding to the first inflection point on the $H_0 - \Delta Y_0/\Delta H_0$ (horizontal load-displacement gradient) curve and $\lg H_0 - \lg Y_0$ (logarithmic of horizontal load vs. displacement) curve. The horizontal ultimate load can be comprehensively determined by considering the horizontal load value corresponding to the starting point of the $H_0 - Y_0$ curve with a significant steep drop, the horizontal load value of the previous level with a significant bend at the tail of the $Y_0 - \lg t$ (logarithmic of displacement vs. time) curve, and the horizontal load value corresponding to the second inflection point on the $H_0 - \Delta Y_0/\Delta H_0$ curve and $\lg H_0 - \lg Y_0$ curve.

The $H_0 - Y_0$, $\lg H_0 - \lg Y_0$, $Y_0 - \lg t$ and $H_0 - \Delta Y_0/\Delta H_0$ curves of test piles S2 and S3 are shown in Fig. 3-6. It can be seen that the $H_0 - Y_0$ curves of test piles S2 and S3 both exhibit gradual deformation. The rebound rate for test pile S2 is 80.92%, with a maximum displacement of 32.18 mm. The rebound rate for test pile S3 is slightly lower, at 75.1%, and its maximum displacement represents 95.72% of that of test pile S2. At a horizontal load of 600 kN, the $Y_0 - \lg t$ curves of test piles S2 and S3 exhibit significant downward bending at the tail. The ultimate horizontal load for both S2 and S3 is 540 kN. Since the allowable value of a single pile's horizontal bearing capacity is only half of its ultimate horizontal bearing capacity, the allowable values for test piles S2 and S3 are both 270 kN, with corresponding displacements of 9.37 mm for S2 and 7.6 mm for S3. When the horizontal load reaches 420 kN, the $H_0 - \Delta Y_0/\Delta H_0$ and $\lg H_0 - \lg Y_0$ curves of test piles S2 and S3 exhibit the first inflection point. The critical horizontal load (H_{cr}) for S2 and S3 is 420 kN, with corresponding horizontal displacements of 17.28 mm for S2 and 14.98 mm for S3. Large- diameter PRC pipe piles are known for their strong bearing capacity and ability to withstand significant horizontal loads. Additionally, under the same horizontal load, test pile S2's pile top displacement will be larger.

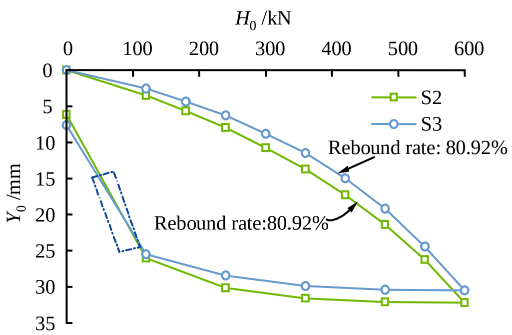

Fig. 3 H_0-Y_0 curves of piles S2 and S3

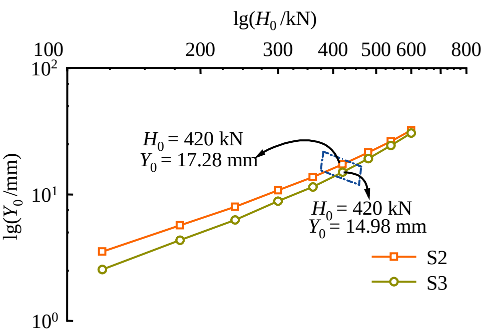

Fig. 4 lgH_0-lgY_0 curves of piles S2 and S3

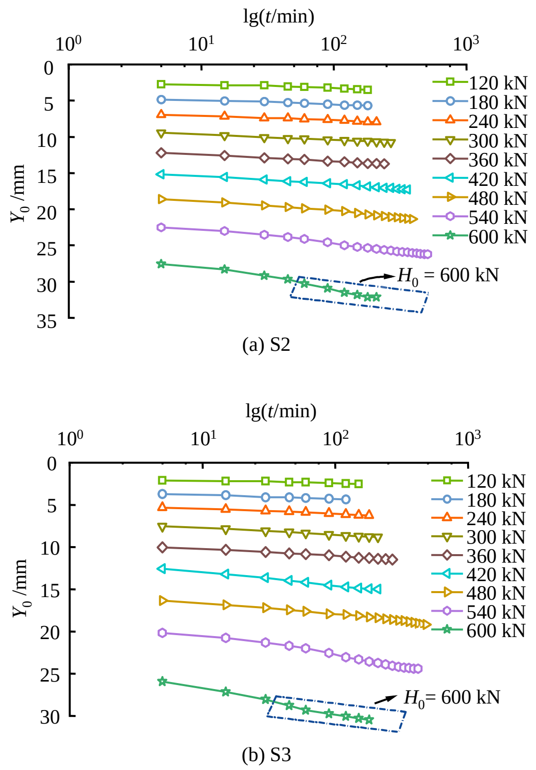

Fig. 5 Y_0-lg$t$ curves of piles S2 and S3 at different H_0

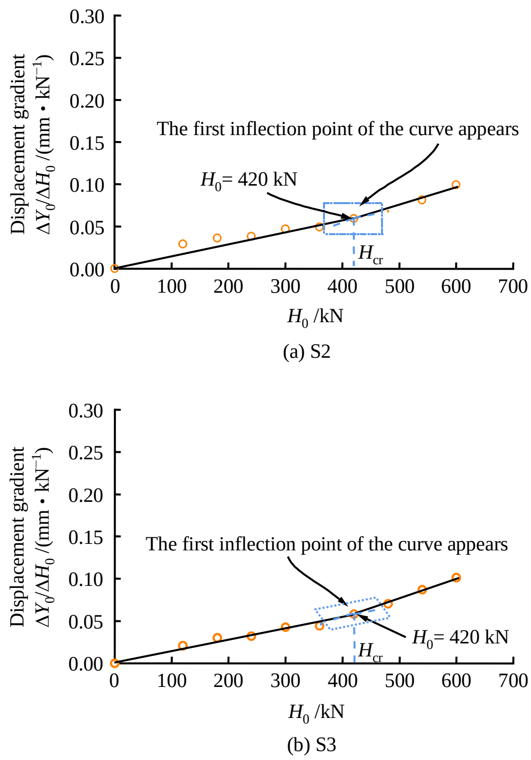

Fig. 6 H_0-$\Delta Y_0/\Delta H_0$ curves of piles S2 and S3

Comparing the horizontal bearing capacities of single piles S2 and S3 across various allowable displacements, significant discrepancies emerge between field-measured values and theoretical calculations based on Eqs. (1) and (2). The ratio of measured to theoretical values falls between 1.78 and 2.21, suggesting that theoretical predictions generally underestimate the actual values. This underestimation is likely due to the complexity of actual soil behavior, which surpasses model assumptions, with features like plastic deformation and anisotropy not adequately represented in the model. Furthermore, the theoretical model may have oversimplified the distribution of friction or cohesion between the pile and soil, neglecting the irregularities of the actual contact surface. Notably, the ratio for pile S3 is significantly higher than that for S2, as shown in Table 2, indicating a greater deviation of S3's conditions or parameters from the theoretical model's assumptions. To reduce errors, it is recommended to employ more complex constitutive models to accurately capture the nonlinear behavior of soil and improve the pile-soil contact assumptions.

Table 2 Comparison between theoretical and measured values of bearing capacity under different allowable displacements

Pile number	Displacement /mm	Theoretical calculation value /kN	Actual measured value /kN	Comparison
S2	6	96.23	188.42	1.96
	8	128.30	242.04	1.89
	10	160.38	285.27	1.78
S3	6	96.23	212.31	2.21
	8	128.30	258.82	2.02
	10	160.38	300.78	1.88

3.1.2 Internal force analysis

Field testing cannot directly determine the bending moment of the pile body. Instead, the distribution of bending moments along the pile body under different load levels must be inferred through strain measurements. Based on beam bending deformation theory and stress analysis, the bending moment at any point on the pile body under horizontal loads can be derived using the equation below:

$$M = \frac{E_c I_z \Delta\varepsilon}{b_0} \quad (3)$$

Where M is the bending moment at any point on the pile body; E_c is the elastic modulus of the pile body; I_z is the moment of inertia; $\Delta\varepsilon$ is the strain difference between two measuring points on the pile section; b_0 is the spacing between tension and compression strain measuring points.

Using Eq. (3), we can calculate the bending moments and maximum bending moments for test piles S2 and S3 at various load levels, as illustrated in Fig. 7. The figure shows that, under the same horizontal load, the bending moment of test pile S2 initially increases to a maximum, then gradually decreases and approaches zero. However, an issue with the steel bar gauge caused the bending moment of test pile S3 to slightly decrease at a depth of 3.6 m, resulting in significant data errors. By analyzing the variation of the bending moment in the test pile, we can observe that the horizontal load at the pile top is primarily supported by the upper pile-soil interface. The soil above the pile plays a crucial role in the horizontal bearing capacity of the pile, whereas the lower section of the pile carries less load. Therefore, in structural design, reinforcing the upper section of the pile can be considered to improve the bending resistance of the pile foundation. The maximum bending moment occurs 5.6 m below the pile top for both test piles, S2 and S3. It indicates that the location of the maximum bending moment remains stable and isn't affected by changes in horizontal load. When the horizontal thrust reaches the ultimate bearing capacity, the maximum bending moment of test pile S2 is 757.14 kN m, which represents 92.13% of the maximum bending moment of test pile S3, demonstrating that large-diameter PRC pipe piles exhibit excellent bending resistance.

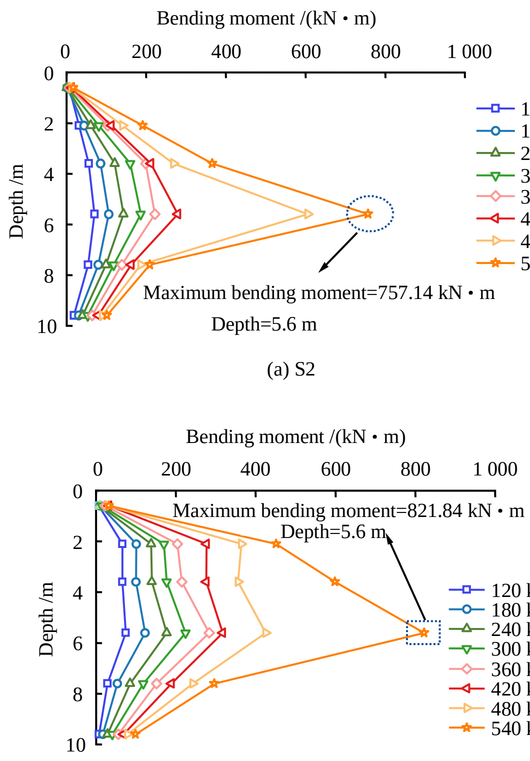

Fig. 7 Bending moment distribution along the pile shaft of a single pile

3.2 Horizontal bearing capacity of a pile cap

3.2.1 Load bearing performance analysis

The H_0-Y_0, $\lg H_0-\lg Y_0$, $Y_0-\lg t$ and $H_0-\Delta Y_0/\Delta H_0$ curves for both the single pile cap and double pile cap are shown in Fig. 8-11. According to Fig. 8, the maximum displacement of a single pile cap is much greater than that of a double pile cap, with a 1.06 times greater maximum displacement. However, the rebound rate of the single pile cap is slightly lower than for the double pile cap, differing by only 1.56%. When the horizontal load reaches 480 kN, the $H_0 - Y_0$ curve of the single pile cap exhibits a significant steep drop, while the $\lg H_0 - \lg Y_0$ curve bends downward notably. The horizontal ultimate load for the single pile cap is 420 kN, which corresponds to a horizontal displacement of 24.65 mm. When the horizontal load reaches 1 400 kN, the $H_0 - Y_0$ curve of the double pile cap exhibits a significant steep drop, whereas the tail of the $\lg H_0 - \lg Y_0$ curve bends downward notably. The horizontal ultimate load for the double pile cap is 1300 kN, which corresponds to a horizontal displacement of 15.02 mm.

The $H_0 - \Delta Y_0/\Delta H_0$ and $\lg H_0 - \lg Y_0$ curves for both the single pile cap and double pile cap exhibit their initial inflection points at horizontal loads of 300 kN and 600 kN, respectively. This implies that the horizontal critical load for the double pile cap is double that of the single pile cap. Because the single pile cap S5 is close to the double pile cap S6-S7, it could impact the test results of the double pile cap, potentially changing their displacement and deformation. Based on the experimental data, the ultimate load difference is 230 kN, while the displacement difference is 9.63 mm. Due to the lateral shielding effect of surrounding piles, the ultimate load capacity of the double pile cap increased by 54.76%, whereas the displacement decreased by 39.07%.

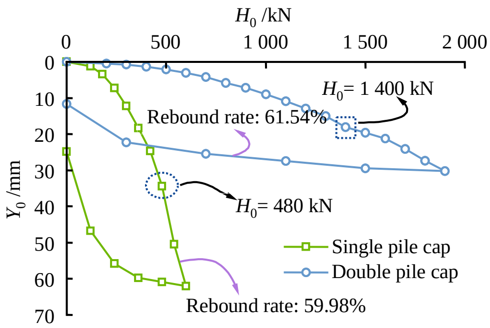

Fig. 8 Horizontal load-displacement curves

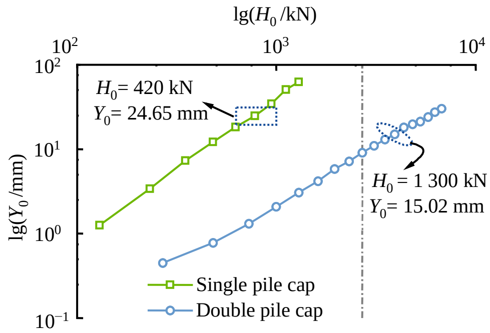

Fig. 9 Double logarithmic curves of horizontal load-displacement

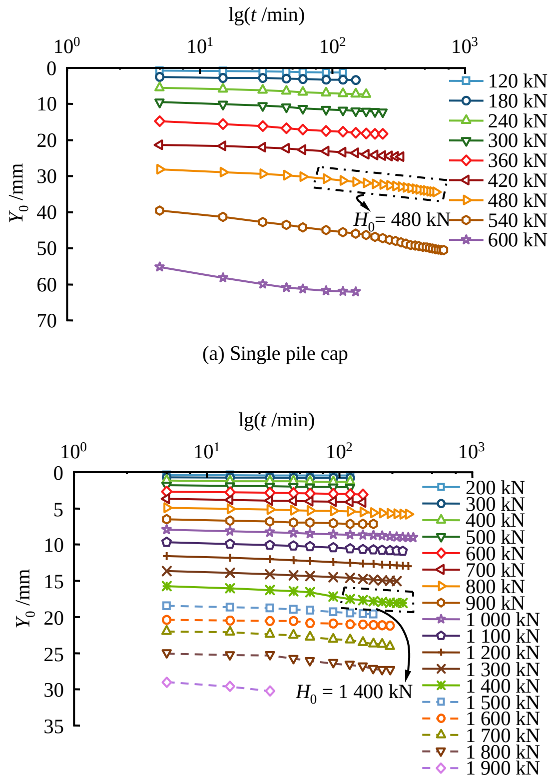

(a) Single pile cap

(b) Double pile cap

Fig. 10 Logarithmic curves of displacement versus time

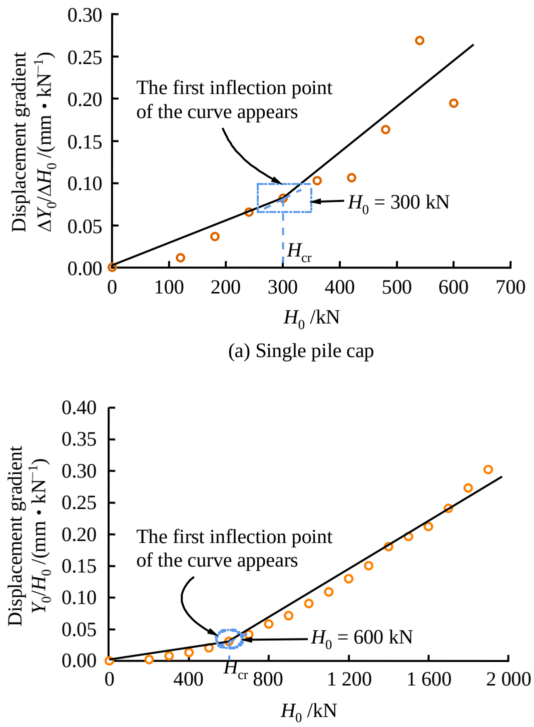

(a) Single pile cap

(b) Double pile cap

Fig. 11 Horizontal load-displacement gradient curves of a pile cap

3.2.2 Internal force analysis

The bending moment curves for single and double pile caps under different loads are shown in Figs. 12 and 13. The maximum bending moment section of a single pile cap is located 4.4 m below the pile top. Under horizontal load, the bending moment at the top of a single pile cap is not zero, unlike the bending moment distribution of a single pile body. Additionally, the presence of the cap changes the bending moment distribution within the pipe pile. The bending moment in the pile body of a double pile cap is primarily concentrated at the upper section, significantly differing from the distribution of a single pile cap. The maximum bending moment section of the double pile cap is just 0.4 m below the pile top, where the front pile S6 experiences a larger bending moment than the rear pile S7. Both the front and rear piles exhibit significant negative bending moments at the top, with the front pile having a larger negative bending moment. The turning point for the front pile's bending moment is located roughly 1.5 m below the pile top, while the rear pile's is approximately 2 m below.

At ultimate load, the maximum bending moment for the single pile cap is 344.47 kN • m. The maximum bending moment of the double pile cap is negative, and the maximum bending moment of the front pile S6 is −621.50 kN • m. The maximum bending moment of the rear pile S7 comprises only 62.37% of the front pile S6's maximum, amounting to −387.64 kN • m. The absolute value of the double pile cap's maximum bending moment exceeds that of the single pile cap, with a deviation of up to 44.57%. Since the front pile S6 is closer to the jack position, it experiences force before the rear pile S7. During loading, the front pile and the soil around it carry a greater portion of the load, whereas the rear pile bears less. Hence, the bending moment of the rear pile's body is less than that of the front pile.

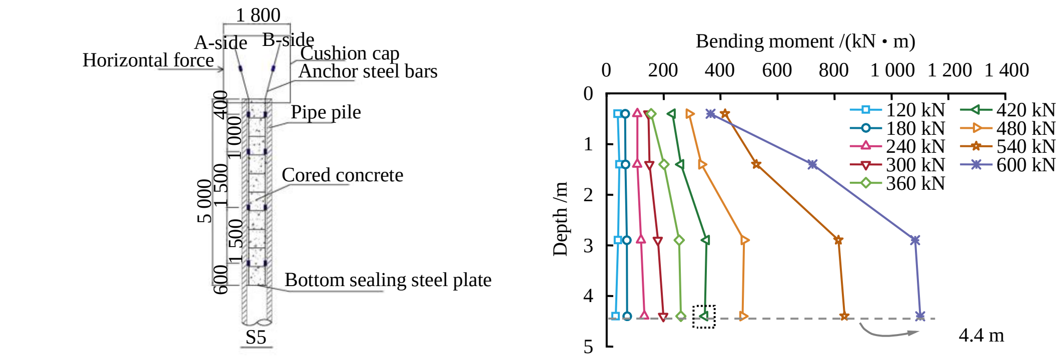

(a) Layout of reinforcement gauge for bearing platform (unit: mm) (b) S5

Fig. 12 Bending moment distribution along the pile shaft of a single pile cap

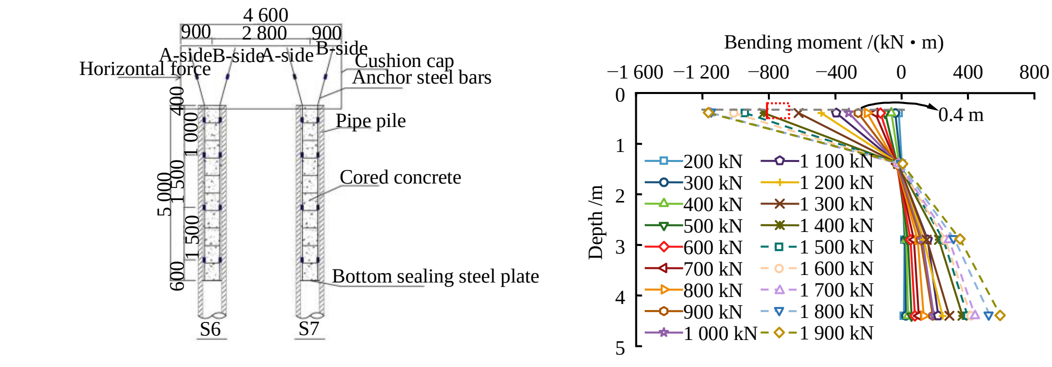

(a) Layout of reinforcement gauge for bearing platform (unit: mm) (b) S6

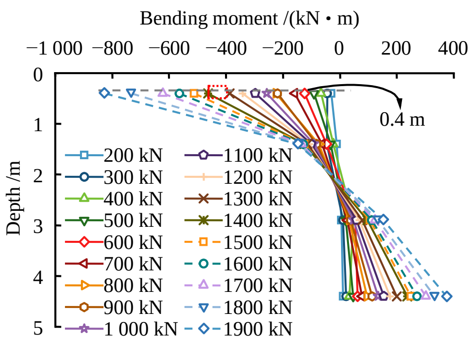

(c) S7

Fig. 13 Bending moment distribution along the pile body of a double pile cap

3.3 Comparative analysis of a single pile versus a pile cap

When comparing the horizontal load-displacement curves of a single pile to those of a single pile with a cap (as shown in Figs. 3 and 8), it is evident that the ultimate horizontal bearing capacity of the pile without a cap is 540 kN. The introduction of a high cap results in a decrease in the horizontal ultimate bearing capacity to 420 kN, representing a 22.22% reduction when compared to the pile without a cap. The horizontal load at the pile top generates a bending moment that leads to a decrease in the pile's horizontal ultimate bearing capacity when a high cap is introduced.

By comparing and analyzing the horizontal load-displacement curves of the single pile cap versus the double pile cap (as shown in Fig. 8), we conclude that as the horizontal load increases, so does the horizontal displacement. Under the same horizontal load, the double pile cap exhibits a smaller horizontal displacement than the single pile cap, with a maximum displacement that is only 48.66% of the single pile cap. Embedding the pile head in the pile cap not only enhances the bending stiffness but also significantly improves the pile foundation's resistance to lateral bending deformation.

From the logarithmic displacement-time curves for single piles and double pile caps (as shown in Fig. 10), we can conclude that the horizontal critical load of the double pile cap is double that of the single pile cap, and the horizontal ultimate load of the double pile cap is 3.095 times greater than that of the single pile cap. Based on the bending moment distribution diagrams for both single and double pile caps (as shown in Figs. 12 and 13), it is evident that the maximum bending moment of the double pile cap is higher than that of the single pile cap, with a deviation ranging from 11.14% to 44.57%.

4 Research on group pile effect

Wu et al. [47] analyzed the impact of pile spacing on the horizontal bearing capacity of pile groups utilizing finite element software and discovered that, when the pile spacing reached 8 D (where D represents the pile diameter), the influence of the pile group effect on the horizontal bearing capacity of the pile groups could be disregarded. In comparison to a single pile, a group pile exhibits substantially distinct stress and deformation characteristics under horizontal loading. Factors such as pile length, spacing between piles, number of piles, pile diameter, arrangement of piles, and the connection between pile top and cap all contribute to the horizontal bearing performance of pile groups. Utilizing ABAQUS, we conduct a comparative analysis of the pile group effects associated with varying thicknesses of pile caps, numbers of piles, and pile spacings, and further investigate the impact on the horizontal bearing capacity of pile groups.

4.1 Model validation

Utilizing ABAQUS, separate finite element back-analyses are conducted for the field test pile S2, a single pile cap, and a double pile cap. A comparative analysis is conducted to compare the finite element analysis results with the field-measured results obtained under horizontal loading conditions. The model's reliability in calculating the horizontal bearing capacity of piles has been verified.

In the finite element model, the foundation soil is modeled using the Mohr-Coulomb elastoplastic constitutive model. Each soil layer is assumed to be an ideal elastoplastic material possessing homogeneous, continuous, and isotropic properties. The soil layer division aligns with the field test results, and the relevant parameter values are presented in Table 1. The pile body's concrete employs a constitutive model based on damage plasticity, matching the C80 concrete used in the field. Table 3 lists the parameters. To minimize boundary effects and adhere to the semi-infinite space assumption of the model, the soil cross-section dimensions (length and width) are set to 20 times the pile diameter, while the soil depth is set to 2 times the pile length. The pile-soil contact adopts the discretization method of Surface-to-Surface in the analysis step of contact. The contact analysis employs the small slip mode, with the normal and tangential behaviors being set for the interfaces between: the bottom surface of the pile cap and the soil interface, the side surface of the pile cap and the pile body interface, and the pile body and soil interface. In the tangential behaviors, the "penalty" friction formula is applied, with a friction coefficient of 0.3.

Table 3 Physical parameters of pile model

Density /(kg · m^{-3})	Elastic modulus /MPa	Poisson's ratio	Expansion angle/(°)	Eccentricity	F_{b0}/F_{c0}
2 500	38 000	0.2	30	0.1	1.16

Note: F_{b0}=concrete biaxial compressive strength; F_{c0} =uniaxial compressive strength of concrete.

Based on the properties of the pile-soil system, the pile body and soil are modeled as three-dimensional reduced integration elements (C3D8R), while the prestressed steel bars are modeled as three-dimensional truss elements (T3D2). When dividing the grid, the soil grid in the horizontal direction near the pile position is densified, radiating outwards, and vertically refined from 1 m to 5 m downwards. Additionally, the grid for the pile body and steel bars is arranged symmetrically as a whole. The lateral and bottom boundaries of the soil are constrained by normal displacement that is perpendicular to the plane. Only when the earth stress is balanced, the pile-soil surface is constrained horizontally. Once equilibrium is achieved, this constraint becomes ineffective.

Fig. 14 demonstrates that the simulation results of field tests conducted using ABAQUS exhibit a high degree of consistency with the measured data, thereby confirming the reliability of ABAQUS in simulating the horizontal bearing capacity of piles.

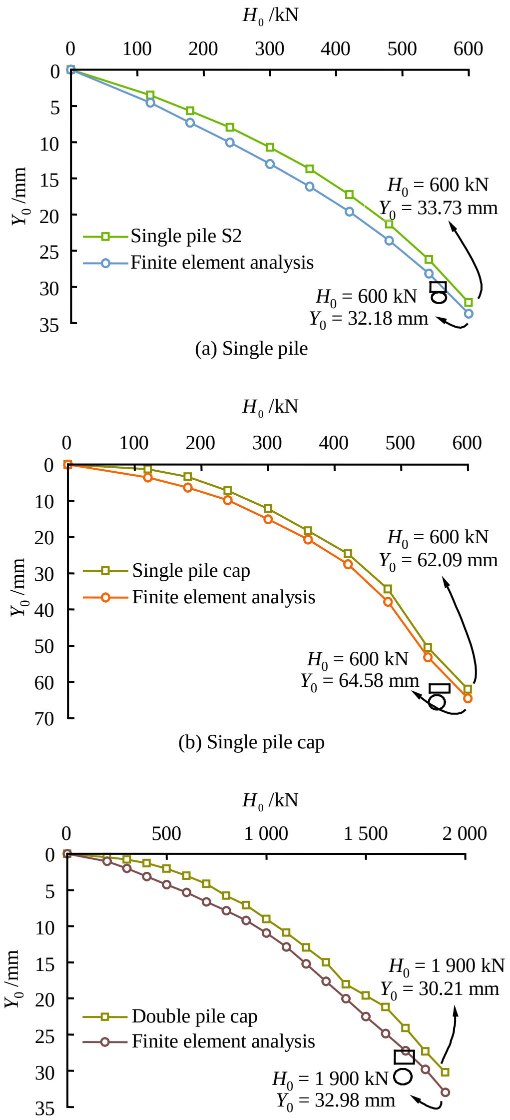

Fig. 14 Comparison of H_0-Y_0 curves between field experiments and finite element simulations

4.2 Working condition settings

In the following operating conditions, the maximum displacement for loading is 30 mm.

（1）Based on the field test of the double pile cap, all other parameters remain unchanged, with the cap size maintained at 1.8 m×4.6 m. Using the double pile cap model, the pile spacing is set at 3.5 *D*, and the cap thicknesses used for calculations are 0.8 m, 1.2 m, 1.5 m, 1.8 m, and 2.0 m.

（2）Based on the field test of the double pile cap, pile length, diameter, spacing, and soil parameters remain unchanged. Models with two, four, six, and nine piles are created for calculation. To ensure even load distribution among pile groups and enhance the foundation's stability and bearing capacity, the pile groups are arranged as follows: two piles in a single row; four, six, and nine piles are arranged in both horizontal and vertical directions, forming symmetrical and balanced pile groups of 2×2, 3×2, and 3×3, respectively.

（3）Based on the field test of the double pile cap, pile length, diameter, and soil parameters remain constant. Utilizing the double pile cap model, models featuring pile spacings of 2.5*D*, 3.5*D*, 4.5*D*, 5*D*, and 6*D* are established for calculation. The setting of pile spacing is determined based on the spacing of 3.5*D* for the double-pile cap on site as the benchmark.

4.3 Result analysis

Lü et al. [48] studied the horizontal bearing capacity of both single and grouped pipe piles, using 75% of the capacity at a 6 mm horizontal displacement as the characteristic value for the basic horizontal bearing capacity. This paper defines the horizontal bearing capacity of the pile group as the load at which the pile top experiences a 10 mm horizontal displacement, and uses this to calculate the comprehensive coefficient of the pile group effect. The pile group effect, resulting from the interaction between the cap, pile group, and soil, is calculated using Eq. (2).

In finite element analysis, the calculation method for the comprehensive coefficient of the pile group effect employs the following equation:

$$\eta = \frac{H_g}{mnH_0} \tag{4}$$

Where H_g and H_0 respectively represent the horizontal bearing capacities of the group pile and the single pile cap at a 10 mm horizontal displacement. *m* and *n* denote the number of longitudinal and transverse piles within the pile group, respectively.

4.3.1 Influence of cap thickness on pile group effect

Using two piles with a fixed spacing of 3.5*D*, the cap thicknesses is calculated as 0.8 m, 1.2 m, 1.5 m, 1.8 m, and 2.0 m. Table 4 displays the comprehensive coefficient of pile group effect calculated using Eq. (4) for various pile cap thicknesses. The table indicates that all comprehensive coefficients of pile group effects exceed 1, yet the impact of varying cap thicknesses on these coefficients is negligible.

Table 4 Comprehensive coefficient of pile group effect under different cap thicknesses

Thickness of cap	0.8 m	1.2 m	1.5 m	1.8 m	2.0 m
η	2.02	1.97	1.92	1.88	1.85

Fig. 15 depicts the horizontal load-displacement curves for different cap thicknesses. At a 10 mm horizontal displacement, the horizontal load for a 0.8 m cap thickness is 1 158.95 kN. Compared to the 0.8 m cap thickness, the horizontal loads for 1.2 m, 1.5 m, 1.8 m, and 2.0 m cap thicknesses decrease by 2.6%, 4.83%, 7.03%, and 8.66%, respectively (as shown in Fig. 16). As the thickness of the pile cap increases, the horizontal bearing capacity experiences a slight decrease. Thicker pile caps alter the bending moment transmission path between the pile and the cap, enabling more effective transfer of horizontal loads to the pile top. Consequently, the pile top bears a greater bending moment, which in turn diminishes the pile's horizontal bearing capacity.

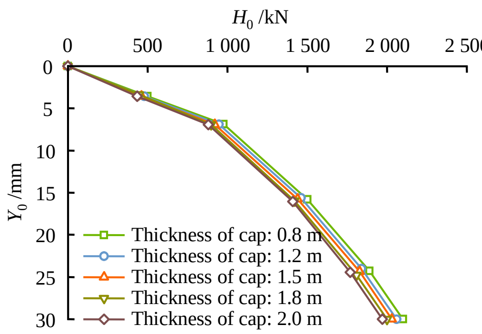

Fig. 15 H_0-Y_0 curves at different cap thicknesses

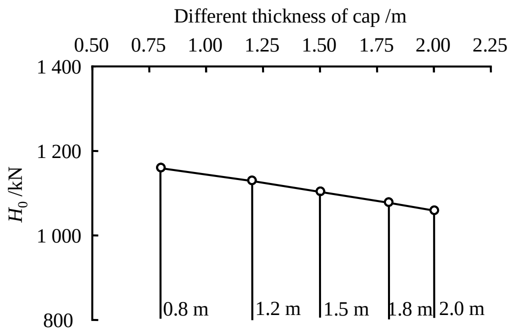

Fig. 16 Horizontal bearing capacity of pile group

4.3.2 Influence of pile number on pile group effect

The pile length, diameter, spacing, and cap size remain constant. Models with two, four, six, and nine piles are established for calculation. The comprehensive coefficient of pile group effect for different numbers of piles is shown in Table 5. As the number of piles increases, the comprehensive coefficient of pile group effect decreases gradually.

The horizontal load-displacement curve under different numbers of piles is shown in Fig. 17. When the horizontal load H_0 =2 000 kN, the horizontal displacement of two piles Y_0 = 30 mm. With four piles, Y_0 decreased by 68.07% to 9.58 mm. With six piles, Y_0 is 7.38 mm, a 22.96% decrease compared to the previous condition. With nine piles, Y_0 = 5.17 mm, which is a decrease of 29.95% compared to the previous condition. As the number of piles increases, the overall bearing capacity of the pile group enhances (as shown in Fig. 18), leading to a more even distribution of load among the piles and minimizing the mutual interference between adjacent piles.

Table 5 Comprehensive coefficient of pile group effect at different numbers of piles

Pile number	2	4	6	9
η	1.85	1.82	1.57	1.38

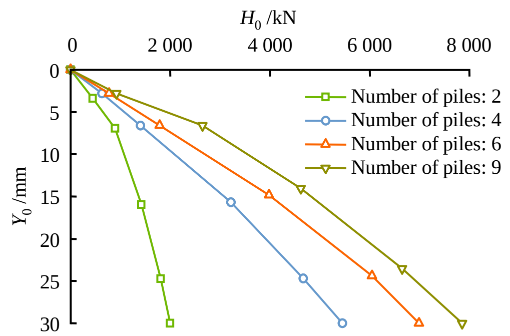

Fig. 17 H_0-Y_0 curves at different numbers of piles

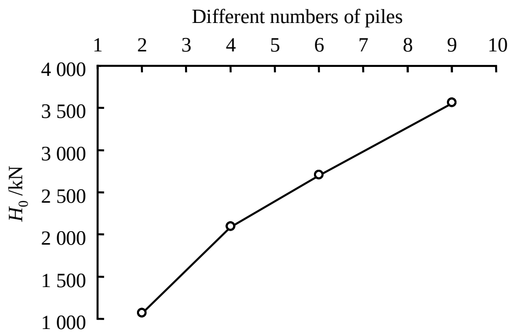

Fig. 18 Horizontal bearing capacity of pile group

4.3.3 Influence of pile spacing on pile group effect

Other parameters remain constant, and models with pile spacing of 2.5*D*, 3.5*D*, 4.5*D*, 5*D*, and 6*D* are established for calculation. Horizontal load- displacement curves have been plotted (as shown in Fig. 19). As shown in Table 6, the comprehensive coefficient of pile group effect increases as pile spacing increases.

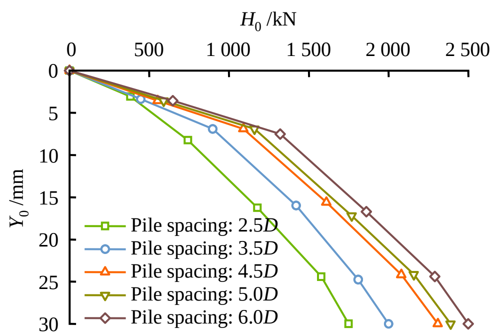

Fig. 19 H_0-Y_0 curves at different pile spacings

Table 6 Comprehensive coefficient of pile group effect at different pile spacings

Pile spacing	2.5*D*	3.5*D*	4.5*D*	5*D*	6*D*
η	1.47	1.85	2.07	2.17	2.3

At a horizontal displacement of 10 mm and a pile spacing of 6*D*, the maximum horizontal load reaches 1 466.31 kN. As pile spacing decreases, the horizontal load diminishes by 8.45%, 12.17%, 27.8%, and 42.81% respectively. As the load on the pile-soil increases, the horizontal bearing capacity of the pile group enhances with increasing pile spacing. When pile spacing exceeds 4.5*D*, the increase in horizontal bearing capacity diminishes (as shown in Fig. 20).

4.3.4 Comparison of comprehensive effect coefficients of pile groups

Table 7 presents a comparison of the comprehensive coefficient of pile group effect between the standard recommendation method and the finite element analysis calculation method. The comprehensive effect coefficients of pile groups, calculated using the finite element analysis method across different pile spacings, numbers, and cap thicknesses, surpass those recommended in the code. Furthermore, the finite element analysis results are approximately 1.17-1.3 times higher than the code-based calculation results.

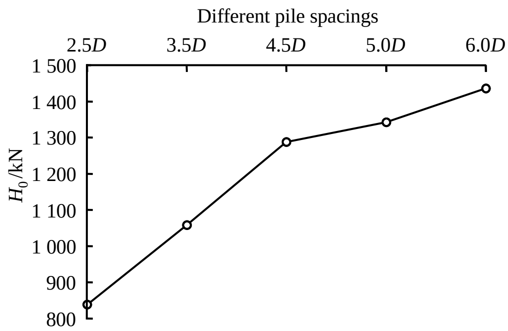

Fig. 20 Horizontal bearing capacity of pile group

Table 7 Comparison of comprehensive coefficients of pile group effect

Pile spacing	η		Pile number	η		Thickness of cap	η	
	Finite element	specification		Finite element	specification		Finite element	specification
2.5*D*	1.47	1.13	2	1.85	1.42	0.8	2.02	1.56
3.5*D*	1.85	1.42	4	1.82	1.40	1.2	1.97	1.52
4.5*D*	2.07	1.73	6	1.57	1.21	1.5	1.92	1.48
5.0*D*	2.17	1.80	9	1.38	1.06	1.8	1.88	1.45
6.0*D*	2.3	1.97	—	—	—	2.0	1.85	1.42

5 Conclusion

This paper undertakes field tests on PRC pipe piles, specifically examining single piles, single pile caps, and double pile caps, and conducts finite element analyses of the foundations comprising these piles and pile caps. The research emphasizes the horizontal bearing characteristics and pile group effects associated with PRC pipe piles, resulting in the following key conclusions:

（1）Under different allowable displacements, the ratio of the theoretical to measured horizontal bearing capacities for single piles S2 and S3 ranges from 1.78 to 2.21. When subjected to the same horizontal loads, the horizontal displacement of a single pile cap is greater than that of a double pile cap, with the maximum displacement being 2.06 times larger. The horizontal critical load of the double pile cap is double that of the single pile cap, while the horizontal ultimate load is 3.095 times greater.

（2）At the ultimate bearing capacities, the maximum bending moment of single pile S2 is 92.13% of that of single pile S3. Regardless of variations in horizontal loads, the position of the maximum bending moment remains stable and consistent.

（3）The presence of the pile cap significantly affects the bending moment distribution of the pipe pile. The bending moment distribution of the double pile cap varies considerably from that of the single pile cap. The maximum bending moment of piles S6 (front row) and S7 (rear row) exceeds the maximum bending moment of the single pile cap by 277.03 kN • m.

（4）As pile spacing increases, the comprehensive effect coefficient of pile groups gradually increases, thereby enhancing the pile group's horizontal bearing capacity. However, when pile spacing surpasses 4.5*D*, the rate of increase begins to decrease. As the number of piles increases, the comprehensive effect coefficient for the pile group drops from 1.85 to 1.38, indicating an overall decrease of approximately 25.4%. Nevertheless, the pile group's overall bearing capacity improves. When the number of piles exceeds six, the decline in the pile group's comprehensive effect coefficient slows down. Variations in cap thickness have minimal influence on the over comprehensive all coefficient of pile group effect.

（5）Using a unified setting of 10 mm horizontal displacement at the pile top as the pile group's horizontal bearing capacity, the comprehensive effect coefficients obtained through the finite element analysis method exceed those recommended in specifications. The standard recommendation method typically relies on extensive engineering experience and experimental data, incorporating a degree of conservatism. Finite element analysis potentially approaches the theoretical limit value more closely.

References

[1] CHEN Rong-bao, ZHANG Ji-chao, CHEN Ze-yu, et al. Study on the vertical bearing mechanism of prestressed pipe piles based on in-situ testing and big data analysis[J]. Building Science, 2022, 38(1): 49−60.

[2] YUE Hong-ya, QI Le, ZHUANG Pei-zhi, et al. Numerical simulation study on key influencing factors of horizontal bearing characteristics of pile groups[J]. Highway, 2015, 60(9): 109−113.

[3] DU Lin. Experimental and theoretical study on new hybrid reinforced prestressed pipe pile for foundation pit support[D]. Zhengzhou: Zhengzhou University, 2012.

[4] GUO Yang, WU Ping, HAN Lei, et al. Experimental and numerical analysis of flexural behavior of prestressed concrete pipe piles with composite reinforcement[J]. Chinese Journal of Underground Space and Engineering, 2019, 15(2): 481−488.

[5] THUSOO S, OBARA T, KONO S, et al. Design models for steel encased high-strength precast concrete piles under axial-flexural loads[J]. Engineering Structures, 2021, 228: 111465.

[6] WU Tong, XU Jian, QIAN Wen-jun, et al. Experimental study on the tensile bearing capacity of pile foundations in permafrost regions[J]. Chinese Journal of Underground Space and Engineering, 2018, 14(1): 145−153.

[7] ZHU Zhao-qing, GONG Wei-ming, DAI Guo-liang. Field experimental study on horizontal bearing capacity of large-diameter steel pipe piles[J]. Building Science, 2010, 26(09): 36−39, 32.

[8] ASHOUR M, NORRIS G, PILLING P. Strain wedge model capability of analyzing behavior of laterally loaded isolated piles, drilled shafts, and pile groups[J]. Journal of Bridge Engineering, 2002, 7(4): 245−254.

[9] GALLI A, PRISCO D. et al. Displacement-based design procedure for slope-stabilizing piles[J]. Canadian Geotechnical Journal, 2013, 50(1): 41−53.

[10] HU H B, LUO L N, LEI G, et al. The transverse bearing characteristics of the pile foundation in a calcareous sand area[J]. Materials, 2022, 15(17): 6176.

[11] KIM S, CHOO W Y, KIM D. Pullout capacity of horizontally loaded suction anchor installed in silty sand[J]. Marine Georesources & Geotechnology, 2016, 34(1): 87−95.

[12] GEROLYMOS N, GIANNAKOS S, DROSOS V. Generalised failure envelope for laterally loaded piles: analytical formulation, numerical verification and experimental validation[J]. Géotechnique, 2020, 70(3): 248−267.

[13] SHI Ji-sen. Study on the efficiency of single row piles under horizontal load[D]. Hangzhou: Zhejiang University of Technology, 2013.

[14] SONG Xiu-guang, YUE Hong-ya, ZHOU Zhi-hong, et al. Numerical simulation study on horizontal bearing characteristics of pile groups[J]. Railway Engineering, 2015, (8): 97−100.

[15] WANG L X, WU W B, EI N M H, et al. Nonlinear analysis of horizontal bearing capacity of large-diameter rigid piles based on double conical strain wedge model[J]. Ocean Engineering, 2023, 285(P2): 115411.

[16] LV C Y, GUO Y C, LI Y H, et al. Experimental study on the horizontal bearing characteristics of long-short-pile composite foundation[J]. Geomechanics and Engineering, 2023, 33(4): 341−352.

[17] DU Bin, LI Xiao-yong, GAO Wen-sheng. Discussion on the estimation formula of single pile horizontal bearing capacity for PHC pipe pile[J]. Industrial Construction, 2023, 53(S2): 451−455.

[18] WAN Zheng, QIU Ren-dong. Study on the horizontal static load characteristics of grouted pile at the pile side and pile end[J]. Chinese Journal of Rock Mechanics and Engineering, 2015, 34(S1): 3588−3596.

[19] DONG Y X, FENG Z J, HU H B, et al. The Horizontal Bearing Capacity of Composite Concrete-Filled Steel Tube Piles[J]. Advances in Civil Engineering, 2020, 2020: 3241602.

[20] LUAN L B, DING X M, ZHENG C J, et al. Dynamic response of pile groups subjected to horizontal loads[J]. Canadian Geotechnical Journal, 2020, 57(4): 469−481.

[21] XU X B, ZHANG T Y, WANG J C, et al. Model tests on the bearing capacity of precast open-ended micro pipe piles in soft soil[J]. Proceedings of the Institution of Civil Engineers-Geotechnical Engineering, 2019, 173(6): 1−56.

[22] LIU Shuo-tian. Numerical analysis of the influence of pier cap on the horizontal bearing capacity of pile groups[D]. Beijing: Beijing Jiaotong University, 2017.

[23] ASHOUR M, ABBAS A I, BOSKOVIC S. Pile cap interaction with bridge pile foundations under lateral loads[J]. Journal of Bridge Engineering, 2019, 24(6) 04019053.

[24] GONG Wei-ming, FU Zhi-qian, WU Jian, et al. Experimental study on horizontal bearing performance of single pile and two pile caps[J]. Bridge Construction, 2013, 43(5): 23−28.

[25] ZHONG Zhao-yin, LENG Wu-ming, YANG Qi, et al.

Horizontal static load test and m value analysis of bridge foundation piles in deep soft soil areas[J]. Journal of Railway Science and Engineering, 2023, 20(9): 3350−3361.

[26] YIN P B, WANG K, CHEN L, et al. Horizontal bearing capacity and reliability of piles in coastal soft soil considering the time-varying characteristics[J]. Journal of Marine Science and Engineering, 2023, 11(2): 247.

[27] THIEKEN K, ACHMUS M, LEMKE K. A new static *p-y* approach for piles with arbitrary dimensions in sand[J]. Geotechnik, 2015, 38(4): 267−288.

[28] SHI Feng, HAO Shi-long. Experimental study on horizontal bearing capacity of PHC piles[J]. Rock and Soil Mechanics, 2015, 36(S2): 617−622.

[29] ZHANG Guo-xun. Experimental and numerical simulation study on horizontal bearing capacity of PHC pipe pile[D]. Xiamen: Huaqiao University, 2012.

[30] DESAI C S. Kuppusamy T, ALAMEDDINE A R. Pile Cap-Pile Group-Soil Interaction[J]. Journal of the Structural Division, 1981, 107(5): 817−834.

[31] DING Cui-hong, WANG Ji-cheng. Numerical simulation analysis of the influence of pier cap on the horizontal bearing capacity of single pile[J]. Journal of Zhejiang University of Technology, 2009, 37(2): 230−235.

[32] ZENG B, ZHANG D W, XU J M, et al. Numerical simulation of horizontal bearing characteristics of cement-soil reinforced rock-socketed steel pipe monopile considering cementation damage[J]. Computers and Geotechnics, 2023, 162: 105626.

[33] BAI Xue. Numerical simulation analysis of the bearing characteristics of PHC pipe piles under horizontal load[D]. Taiyuan: Taiyuan University of Technology, 2021.

[34] HUANG Xiao-long, GUO Zhao-sheng, HE Wu-bin, et al. Finite element analysis of horizontal stress characteristics of PHC pipe piles and pipe piles with abutments[J]. Concrete, 2016(9): 117−119, 127.

[35] WANG An-hui, ZHANG Ding-wen, LIU Song-yu, et al. Study on the bearing characteristics of steel composite pipe piles under horizontal load[J]. Journal of China University of Mining and Technology, 2018, 47(4): 853−861.

[36] ZHAO Chun-feng, WANG Wei-zhong, ZHAO Cheng, et al. Experimental study on the horizontal bearing characteristics of a single pile under vertical and bending moment loads in sandy soil[J]. Chinese Journal of Rock Mechanics and Engineering, 2013, 32(1): 184−190.

[37] LEI Hua-yang, LIU Li-xia, HUO Hai-feng, et al. Study on load transmission characteristics and bearing capacity of high cap pipe pile under horizontal load[J]. Building Science, 2012, 28(5): 20−25, 29.

[38] HONG J, WEI K, SHEN Z H, et al. Experimental study of breaking wave loads on elevated pile cap with rectangular cross-section[J]. Ocean Engineering, 2021, 227: 108878.

[39] XU B, WEI K, QIN S Q, et al. Experimental study of wave loads on elevated pile cap of pile group foundation for sea-crossing bridges[J]. Ocean Engineering, 2020, 97: 106896.

[40] ZHANG J R, WEI K, LI J Z. Integrated assessment of the hydrodynamic added mass of the deep-water pile-cap foundation considering pile group-pile cap interaction[J]. Ocean Engineering, 2022, 244: 110418.

[41] FRANCA A G, RODRIGO G J. Influence of Pile Cap-Ground Contact Geometry on the Behavior of Piled Foundations[J]. Arabian Journal for Science and Engineering, 2023, 48(10): 14029−14041.

[42] ZHAO C, SRI S, JERAMY C A. Behavior of a Pile Group Supporting a Precast Pile Cap under Combined Vertical and Lateral Loads[J]. Journal of Geotechnical and Geoenvironmental Engineering, 2021, 147(9): 04021084.

[43] LING X Z, HAO L, SHUN C X, et al. Study on seismic response of liquefiable soil-pile group considering pile cap and soil contact[J]. Soil Dynamics and Earthquake Engineering, 2024, 183: 108827.

[44] MA R J, LIU Y, CHANG H C, et al. Effect of Square Cap on Pile-Group Wave Force: Parametric Analysis and Case Study[J]. Journal of Marine Science and Engineering, 2023, 11(9): 1677.

[45] China Academy of Building Research. JGJ94－2008 Technical code for building pile foundations[S]. Beijing: China Architecture & Building Press, 2008.

[46] Traffic Engineering Management Center of Zhejiang Province. JTG/T 3512－2020 Technical specification for piles testing of highway engineering[S]. Beijing: People's Communications Publishing House, 2020.

[47] WU Yu-ping, FU Hong-an, WANG Jia-jia, et al. Study on the horizontal bearing capacity and group pile effect of micro piles in loess foundation[J]. Chinese Journal of Applied Mechanics, 2022, 9(3): 543−553.

[48] LÜ Duo, XIE Feng, CHEN Pei, et al. Horizontal bearing performance test of PHC pipe piles and pile groups for transmission lines[J]. Building Structure, 2020, 50(17): 132−137.